BIOCHEMICAL PHARMACOLOGY 74 (2007) 1078–1090

available at www.sciencedirect.com

ScienceDirect

journal homepage: www.elsevier.com/locate/biochempharm

Ursolic acid ameliorates cognition deficits and attenuates oxidative damage in the brain of senescent mice induced by D-galactose

Jun Lu [a,b], *Yuan-Lin Zheng* [a,*], *Dong-Mei Wu* [a], *Lan Luo* [c], *Dong-Xu Sun* [a], *Qun Shan* [a]

[a] *Key Laboratory for Biotechnology on Medicinal Plants of Jiangsu Province, Xuzhou Normal University, Xuzhou 221116, PR China*
[b] *Institute of Molecular Medicine and Genetics Research Center, School of Basic Medical Science, Southeast University, Nanjing 210009, PR China*
[c] *Department of Biological Science and Technology, Nanjing University, Nanjing 210093, PR China*

ARTICLE INFO

Article history:
Received 11 June 2007
Accepted 2 July 2007

Keywords:
Ursolic acid
D-Galactose
ROS
Behavior
Antioxidant enzyme
Caspase-3
GAP43

ABSTRACT

Ursolic acid (UA), a pentracyclic triterpene, is reported to have an antioxidant activity. Here we assessed the protective effect of UA against the D-galactose (D-gal)-induced neurotoxicity. We found that UA markedly reversed the D-gal induced learning and memory impairment by behavioral tests. The following antioxidant defense enzymes were measured: superoxide dismutases (SOD), catalase (CAT), glutathione peroxidase (GPx) and glutathione reductase (GR). The content of the lipid peroxidation product malondialdehyde (MDA) was also analyzed. Our results indicated that the neuroprotective effect of UA against D-gal induced neurotoxicity might be caused, at least in part, by the increase in the activity of antioxidant enzymes with a reduction in lipid peroxidation. And UA also inhibited the activation of caspase-3 induced by D-gal. Furthermore, we found that UA significantly increased the level of growth-associated protein GAP43 in the brain of D-gal-treated mice. These results suggest that the pharmacological action of UA may offer a novel therapeutic strategy for the treatment of age-related conditions.

1. Introduction

Formation of reactive oxygen species (ROS) has been proposed to be an important step leading to neuronal death in a variety of age-related neurodegenerative disorders such as Alzheimer's disease and Parkinson's disease [1–3]. The neuron is particularly susceptible to oxidative damage resulted from the production of ROS. ROS oxidizes various biological macromolecules thereby disturbing homeostatics within the neuron and ultimately resulting in cell death. D-Galactose (D-gal) can cause the accumulation of ROS, or stimulate free radical production indirectly by the formation of advanced glycation endprodcts (AGE) in vivo, finally resulting in oxidative stress [4]. Mice injected with D-gal have been used for pharmacological studies. Further studies showed that D-gal induced aging-related changes included increased production of free radicals and decreased antioxidant enzyme activities [4,5]. Recent studies have also demonstrated that continuous subcutaneous injection of D-gal in mice induced an increase in cell karyopyknosis, apoptosis and caspase-3 protein levels in hippocampal neurons [6].

* *Corresponding author*. Tel.: +86 516 83500348; fax: +86 516 83500348.
E-mail addresses: ylzheng@xznu.edu.cn, yzheng170@yahoo.com.cn (Y.-L. Zheng).

Abbreviations: CAT, catalase; Ctrl, control; D-gal, D-galactose; GAP43, growth associated protein 43; GR, glutathione reductase; GPx, glutathione peroxidase; MDA, malondialdehyde; SOD, superoxide dismutases; UA, Ursolic acid

0006-2952/$ – see front matter © 2007 Elsevier Inc. All rights reserved.
doi:10.1016/j.bcp.2007.07.007

Drugs isolated from traditional medicinal plants may provide a promising therapy on brain injuries caused by oxidative stress. Ursolic acid (UA; 3β-hydroxy-urs-12-en-28-oic acid) is a triterpenoid compound, which is widely present in berries, leaves, flowers, and many kinds of medicinal herbs, such as *Perilla frutescens* [7], *Glechoma hederaceae* [8], *Rosemarinus officinalis*, and *Eriobotrya japonica* [9], in the form of free acid or as aglycones of triterpenoid saponins [10]. This triterpenoid compound has been reported to induce pleiotropic biological activities such as anti-tumor, antioxidant, anti-inflammatory, hepatoprotective, anti-ulcer, antimicrobial, anti-hyperlipidemic and antiviral [11–15]. Shih et al. studied the protective effect of ursolic acid on the hippocampal neurons against kainate-induced excitotoxicity in rats and proved that free radical scavenging may account, at least partially, for the protective effects of ursolic acid [16]. However, no work has been done to study whether UA has an effect against D-gal induced neurotoxicity in mice model. In the present report, we addressed this issue and investigated the mechanism underlying the neuroprotective effect of UA.

2. Materials and methods

2.1. Subjects

Ten-week-old male Kunming strain mice (29.85 ± 5.58 g) were purchased from the Branch of National Breeder Center of Rodents (Shanghai, China). Prior to experiments the mice had free access to food and water and were kept under constant conditions of temperature (23 ± 1 °C) and humidity (60%). Ten mice were housed per cage on a 12-h light/12-h dark schedule (lights on 08:30–20:30 h). After acclimatization to the laboratory conditions, two groups of mice received daily subcutaneous injection of D-gal (Sigma–Aldrich, MO, USA) at dose of 50 mg/(kg day) for 8 weeks, and the third group served as vehicle control with injection of saline (0.9%) only. Then one group of D-gal-treated mice received ursolic acid (Sigma–Aldrich) of 10 mg/(kg day) in distilled water containing 0.1% Tween-80 (dH_2O/0.1% Tween-80) by oral gavage, for another 2 weeks. Meanwhile, the other group of D-gal-treated mice and the vehicle control were given dH_2O/0.1% Tween-80 without ursolic acid. All experiments were performed in compliance with the Chinese legislation on the use and care of laboratory animals and were approved by the respective university committees for animal experiments. After the behavioral testing, mice were sacrificed and brain tissues were immediately collected for experiments or stored at −70 °C for later use.

2.2. Behavioral tests

2.2.1. Open field test

Each mouse was placed in the center of an open field chamber with internal dimensions of 50 cm × 50 cm and walls of 30 cm high, illuminated by a 40-W bulb (3000 lux) placed 2.8 m above the center of it. The open field was divided into 21 equally sized squares by white lines. Tests were performed in the breeding room from 8:30 to 16:00 h. After 1-min adaptation, the behavior of each mouse was recorded for 5 min by two observers 1 m away from the open field area. Between trials, the mice were returned to their home cage in the same room and the open field was wiped clean with a slightly damp cloth. The behavioral parameters recorded were: (1) ambulation: the number of grids crossed in the arena during the observation period; (2) rearing: the number of times the mouse stood on its hind legs; (3) leaning: the number of times the mouse placed one or two forelimbs on the wall of the arena; (4) grooming: the number of times the mouse 'washed' itself by licking, wiping, combing, or scratching any part of the body.

2.2.2. Morris water maze

The Morris water maze test was performed as described previously [17]. The experimental apparatus consisted of a circular water tank (100 cm in diameter, 35 cm in height), containing water (23 ± 1 °C) to a depth of 15.5 cm, which was rendered opaque by adding ink. A platform (4.5 cm in diameter, 14.5 cm in height) was submerged 1 cm below the water surface and placed at the midpoint of one quadrant. The pool was located in a test room, which contained various prominent visual cues. Each mouse received four training periods per day for 4 consecutive days. Before the first trail, each mouse was put on the platform for 15 s, and then it was given a 30 s free swim and then was assisted to the platform where it was remained for another 15 s rest. For each trial, the mouse was placed in the water facing the wall at one of four starting positions, and the time required for the released mouse to find the hidden platform was recorded. A mouse that found the platform was allowed to remain on the platform for 15 s and then returned to its cage for the inter-trial interval. A mouse that did not find the platform within 60 s was placed on the platform for 15 s at the end of the trial. Latency to escape from the water maze (finding the submerged escape platform) was calculated for each trial. On day 5, the probe test was carried out by removing the platform and allowing each mouse to swim freely for 60 s. The time that mice spent swimming in the target quadrant (where the platform was located during hidden platform training), and in the three non-target quadrants (right, left, and opposite quadrants), was measured, respectively. For the probe trials, the number of times crossing over the platform site was measured and calculated. All data were recorded with a computerized video system.

2.3. Preparation of tissue samples

2.3.1. Tissue homogenates

For biochemical studies, animals were deeply anesthetized and sacrificed. Brains were promptly dissected and perfused with 50 mM (pH 7.4) ice-cold phosphate buffer saline solution (PBS). Brains were homogenized in 1/5 (w/v) PBS containing a protease inhibitor cocktail (Sigma–Aldrich) with 10 strokes at 1200 rpm in a Potter homogenizer. Homogenates were divided into two portions and one part was directly centrifuged at 8000 × *g* for 10 min to obtain the supernatant. Supernatant aliquots were used to determine brain catalase (CAT), glutathione peroxidase (GPx), glutathione reductase (GR) activities, MDA levels and protein contents. The second part of homogenates was sonicated four times for 30 s with 20 s intervals using a VWR Bronson Scientific sonicator, centrifuged at 5000 × *g* for 10 min at 4 °C, and the supernatants were

collected and stored at −70 °C for determination of superoxide dismutases (SOD) enzyme activities. Protein contents were determined by using the BCA assay (Pierce Biotechnology, Inc., Rockford, IL, USA).

2.3.2. Collection of brain slice

For in situ hybridization studies, the mice were perfused transcardially with 25 ml of normal saline (0.9%). The brain tissues were fixed in a fresh solution of 4% paraformaldehyde (pH 7.4) for 4 h, incubated overnight at 4 °C in 100 mM sodium phosphate buffer (pH 7.4) containing 30% sucrose; and embedded in Optimal Cutting Temperature (OCT, Lecia, CA, Germany). Cryosections (12 μm) were collected on 3-amino-propyl-trimethoxysilane-coated slides (Sigma–Aldrich) and stored at −70 °C.

2.4. Measurement of antioxidative systems and oxidative products

2.4.1. Assay of Cu, Zn-SOD activity

Chemicals used in the assay, including xanthine, xanthine oxidase, cytochrome *c*, bovine serum albumin (BSA) and SOD, were purchased from Sigma Chemical Company (St. Louis, MO, USA). Cu, Zn-SOD activity was measured according to the method described by McCord and Fridowich [18]. Solution A was prepared by mixing 100 ml of 50 mM PBS (pH 7.4) containing 0.1 mM EDTA and 2 μmol of cytochrome *c* with 10 ml of 0.001N NaOH solution containing 5 μmol of xanthine. Solution B contained 0.2 U xanthine oxidase/ml and 0.1 mM EDTA. Fifty microliters of a tissue supernatant was mixed with 2.9 ml of solution A and the reaction was started by adding 50 μl of solution B. Change in absorbance at 550 nm was monitored in a spectrophotometer (Shimadzu UV-2501PC, Japan). A blank was run by replacing the supernatant with 50 μl of ultra pure water. Cu, Zn-SOD levels were expressed as units per mg protein with reference to the activity of a standard curve of bovine copper-, zinc-SOD under the same conditions.

2.4.2. Assay of CAT activity

CAT activity was assayed by the method of Aebi [19]. In brief, to a quartz cuvette, 0.65 ml of the phosphate buffer (50 mmol/l; pH 7.0) and 50 μl sample were added, and the reaction was started by addition of 0.3 ml of 30 mM hydrogen peroxide (H_2O_2). The decomposition of H_2O_2 was monitored at 240 nm at 25 °C. CAT activity was calculated as nM H_2O_2 consumed/min/mg of tissue protein.

2.4.3. Assay of GPx activity

The GPx activity assay was based on the method of Paglia and Valentine [20]. *tert*-Butylhydroperoxide was used as substrate. The assay measures the enzymatic reduction of H_2O_2 by GPx through consumption of reduced glutathione (GSH) that is restored from oxidized glutathione GSSG in a coupled enzymatic reaction by GR. GR reduces GSSG to GSH using NADPH as a reducing agent. The decrease in absorbance at 340 nm due to NADPH consumption was measured in a Molecular Devices M2 plate reader (Molecular Devices, Menlo. Park, CA). GPx activity was computed using the molar extinction coefficient of 6.22 $mM^{-1}\,cm^{-1}$. One unit of GPx was defined as the amount of enzyme that catalyzed the oxidation of 1.0 μmol of NADPH to $NADP^+$ per minute at 25 °C.

2.4.4. Assay of GR activity

The GR activity assay was based on the method of Mizuno and Ohta [21]. The enzymatic activity was assayed photometrically by measuring NADPH consumption. In the presence of GSSG and NADPH, GR reduces GSSG and oxidizes NADPH, resulting in a decrease of absorbance at 340 nm, which was measured in a M_2 plate reader. Quantification was based on the molar extinction coefficient of 6.22 $mM^{-1}\,cm^{-1}$ of NADPH. One unit of GR was defined as the amount of enzyme that reduced 1 μmol of GSSG (corresponding to the consumption of 1 μmol of NADPH) per minute at 25 °C.

2.4.5. Measurement of malondialdehyde (MDA) levels

Chemicals, including *n*-butanol, thiobarbutiric acid, 1,1,3,3-tetramethoxypropane and all other reagents, were purchased from Sigma Chemical Company (St. Louis, MO, USA). The level of malondialdehyde (MDA) in brain tissue homogenates was determined using the method of Uchiyama and Mihara [22]. Half a milliliter of each homogenate was mixed with 3 ml of H_3PO_4 solution (1%, v/v) followed by addition of 1 ml of thiobarbituric acid solution (0.67%, w/v). The mixture was incubated at 95 °C in a water bath for 45 min. The colored complex was extracted into *n*-butanol, and the absorption at 532 nm was measured using tetramethoxypropane as standard. MDA levels were expressed as nmol per milligram of protein.

2.5. Immunohistochemistry

Mouse tissues were sectioned after being fixed in 4% paraformaldehyde. For immunohistochemistry, endogenous peroxidase activity in the sectioned tissues was blocked with 3% H_2O_2, and nonspecific binding sites were blocked with 3% normal goat serum (Chemicon International Inc., Temecula, CA). The sections were incubated with anti-cleaved caspase-3 (1:50, Cell Signaling Technology, Inc., Beverly, MA, USA) in Tris-buffered saline (TBS) containing 1% goat serum at 4 °C overnight. Subsequently, biotinylated goat anti-rabbit IgG secondary antibody (diluted as per the recommendations of the supplier; Vector Laboratories, Inc., Burlingame, CA, USA) was applied, followed by incubation for 1 h with an avidin–biotin–horseradish peroxidase complex (ABC Elite Kit, Vector Laboratories, Inc.). Horseradish peroxidase was reacted with diaminobenzidine and H_2O_2 for 5 min to yield a permanent deposit. Stained whole mounts were rinsed in distilled water, mounted on 3-aminopropyl-trimethoxysilane-coated slides, air-dried overnight, dehydrated in ethanol, cleared in xylene, and cover-slipped with cytoseal (Stephens Scientific, Kalamazoo, MI). The specificity of the staining was assessed by omitting the primary antibody.

2.6. In situ hybridization

2.6.1. RNA isolation, RT-PCR, plasmid construction and in vitro synthesis of riboprobes

Whole brains of mice were dissected after euthanasia with an overdose of the anesthetic agent. Total mRNA was extracted

from mice brain with Trizol (Invitrogen, Carlsbad, CA, USA). About 50–100 mg of brain material was used for RNA isolation with 1 ml of Trizol Reagent. AMV reverse transcriptase (Promega, Madison, WI, USA), and oligo-(dT)15 primers (Promega) were used for generating total cDNA. PCR cloning of growth-associated protein GAP43 was performed with primers containing EcoRI and BamHI (New England Biolab, Beverly, MA) restriction enzyme cut site. The sequences of PCR primers were as follows:

- 5′-ATCGAATTCATGGCTCTGCTACTACCG -3′(forward primer);

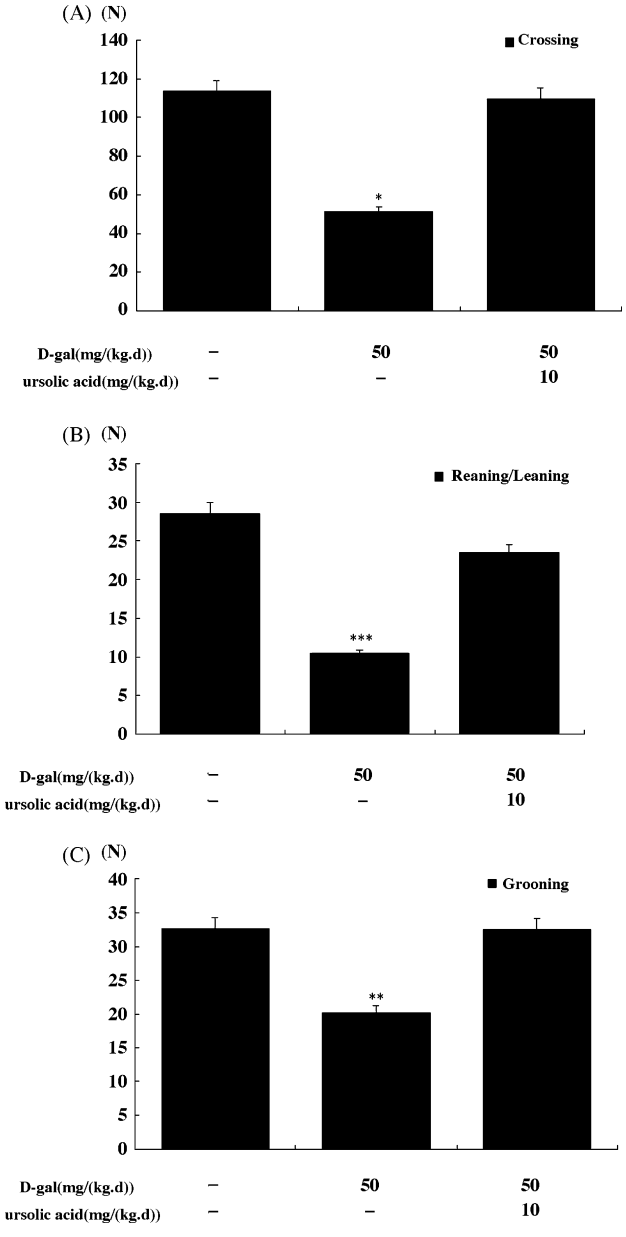

Fig. 1 – Number of line crossing, rearing/leaning and self-grooming in the open field test in the vehicle controls, D-gal-treated mice and D-gal-treated mice fed with UA. Each value is the mean ± S.E.M. $^{*}P < 0.05$; $^{**}P < 0.01$; $^{***}P < 0.001$ as compared to the control group.

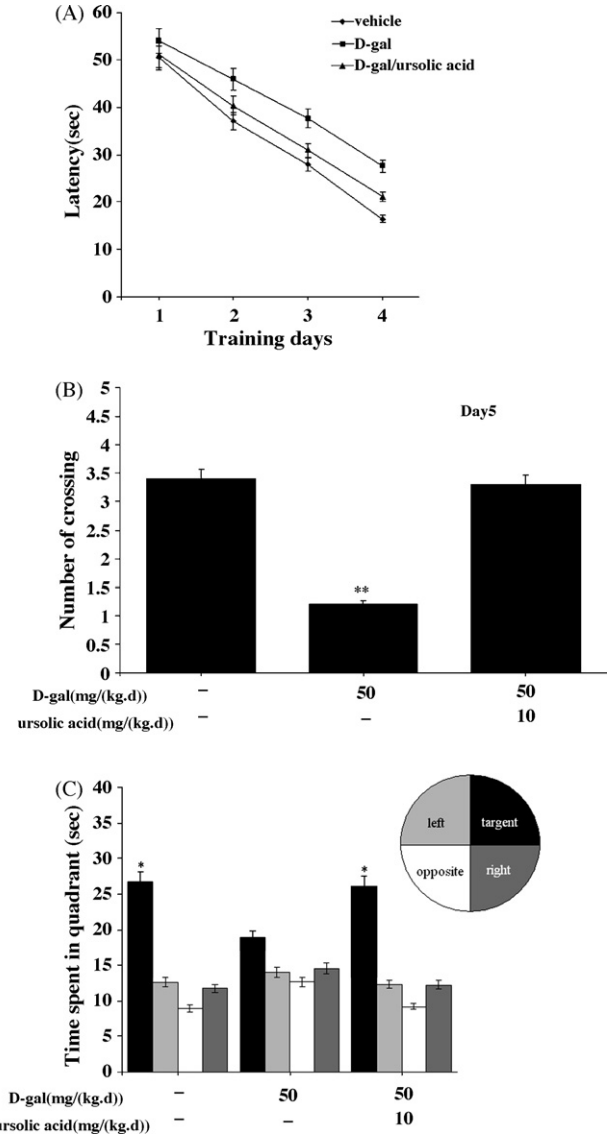

Fig. 2 – Spatial learning and memory in the Morris water-maze test. (A) Mean latency in the hidden platform test; (B) the number of crossings over the exact location of the former platform. $^{**}P < 0.01$ as compared to the control group; (C) comparison of the time spent in target quadrant with other quadrants on day 5. $^{*}P < 0.05$ as compared to any other quadrant.

- 5′-ATCGGATCCGCTTCGTCTACAGCGTCT -3′(reverse primer).

PCR was performed in 50 μl containing thermostable High-Fidelity Taq DNA polymerase (Roche Diagnostics Corporation, Indianapolis, IN, USA), which provides a 3′ to 5′ proofreading activity, 0.1 mM dNTPs and 1 mM $MgCl_2$, using the Expand High-Fidelity PCR-system according to the instructions of the manufacturer. For PCR, the initial melting temperature was 95 °C for 5 min, followed by 35 cycles at 94 °C for 30 s, 55 °C for 30 s, and 72 °C for 1 min, with a final extension at 72 °C for 10 min. The PCR products were visualized on a 1% agarose gel and purified with a Wizard SV Gel and PCR Clean-Up System

kit (Promega) and cloned into pGEM3Z plasmids (Promega). The insert was sequenced and verified to be a 364 base-pair (bp) cDNA, corresponding to bases 400–763 of the GAP43 mRNA. To make GAP43 riboprobe templates, the recombinant plasmid containing the 364 bp GAP43 cDNA fragment was linearized with EcoRI and transcribed with SP6 to generate a complementary RNA (cRNA) antisense probe complementary to mouse GAP43 mRNA. A sense probe was generated by linearizing the plasmids with BamHI, and transcribed with T7 RNA polymerase. Antisense and sense (control) riboprobes were labelled during in vitro transcription in a reaction mixture containing DIG RNA Labeling mix (Roche Diagnostics Corporation), 1 μg of linearized plasmids, and 20 units of SP6 or T7 RNA polymerase (Promega) according to the manufacturer's protocol. After transcription, the template DNA was digested with 40 units of DNase I for 15 min at 37 °C. Unincorporated labeling molecules were removed by centrifugation.

2.6.2. Brain sections in situ hybridization

The in situ hybridization procedure was carried out as described (Roche Diagnostics Corporation), all steps being performed in RNAse-free conditions. Briefly, the frozen mouse brain sections were arranged in metal racks and brought to room temperature for 30 min. The sections were fixed for 10 min with a 4% paraformaldehyde solution in PBS, rinsed twice with PBS and twice with PBS containing 100 mM glycine, permeabilized for 30 min at 37 °C with TE buffer [100 mM Tris–HCl, 50 mM EDTA, pH 8.0] containing 20 μg/ml RNase-free proteinase K (Merck, Darmstadt, Germany), post-fixed for 5 min at 4 °C with DEPC-treated PBS containing 4% paraformaldehyde, acetylated with 0.25% acetic-anhydride in 0.1 M triethanolamine–HCl (pH 8.0) for 15 min and dehydrated through graded ethanol. The sections were equilibrated for 5 min in 4 × SSC, and then prehybridized for 2 h at 55 °C in 4 × SSC containing 50% deionized formamide (Ameresco). Hybridization was performed at 60 °C overnight in hybridization buffer solution containing 40% deionized formamide (Ameresco Co., Solon, OH, USA), 400 ng/ml digoxigenin-labeled probes, 10% dextran sulfate (Sigma–Aldrich), 1 × denhard's solution [0.02% Ficoll-400 (Ameresco Co.), 0.02% polyvinylpyrrolidone (Ameresco Co.), 10 mg/ml RNase-free bovine serum albumin (Ameresco Co.)], 4 × SSC, 10 mM DTT (Sigma–Aldrich), 1 mg/ml yeast tRNA (Calbiochem, La Jolla, CA), and 1 mg/ml denatured and sheared salmon sperm DNA (Sigma–Aldrich). Prior to hybridization, the riboprobes were denatured for 5 min at 80 °C and then cooled on ice. Following hybridization, the sections were washed three times for 1 h each with 2 × SSC at room temperature, 2 × SSC at 65 °C and 0.1 × SSC at 65 °C, respectively. Slides were then incubated for 1 h in 0.5% blocking reagent (Roche Diagnostics Corporation) prepared in 150 mM NaCl, 100 mM Tris–HCl pH 7.5 (NT), and the localization of the bound riboprobes was detected by incubating overnight at 4 °C with an AP-coupled anti-digoxigenin antibody (Roche Diagnostics Corporation) diluted 1:2000 in 0.5% blocking reagent prepared in NT. The slides were washed twice in NT and equilibrated in a solution of 50 mM $MgCl_2$, 100 mM NaCl and 100 mM Tris–HCl pH 9.5 (MNT). The antibody was visualized using an alkaline phosphatase substrate (338 μg/ml nitroblue tetrazolium, 175 μg/ml 5-bromo-4-chloro-3-indolyl phosphate; Roche Diagnostics Corporation) in MNT buffer. Finally, the color reaction was stopped by washing the slides with 10 mM Tris–HCl (pH 8.0) containing 1 mM EDTA.

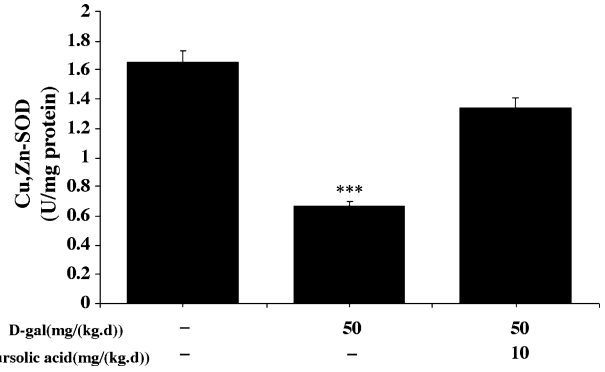

Fig. 3 – Effect of ursolic acid on the Cu, Zn-SOD activity in the brain of D-gal-treated mice. Each value is the mean ± S.E.M. ***P < 0.001, as compared to the control group.

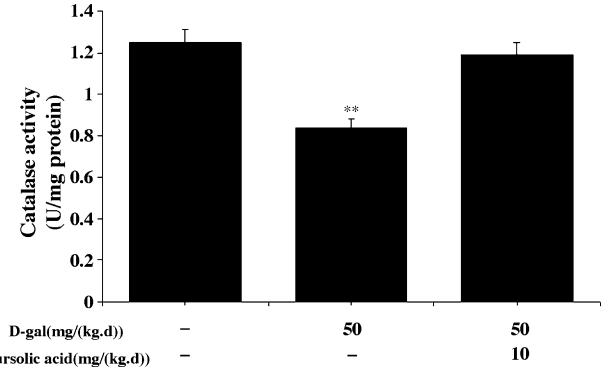

Fig. 4 – Effect of ursolic acid on the CAT activity in the brain of D-gal-treated mice. Each value is the mean ± S.E.M. **P < 0.01, as compared to the control group.

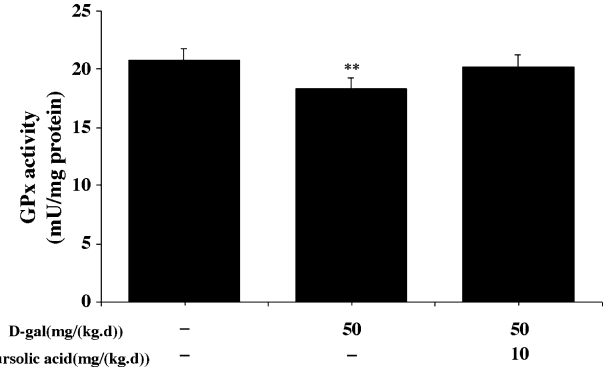

Fig. 5 – Effect of ursolic acid on the GPx activity in the brain of D-gal-treated mice. Each value is the mean ± S.E.M. **P < 0.01, as compared to the control group.

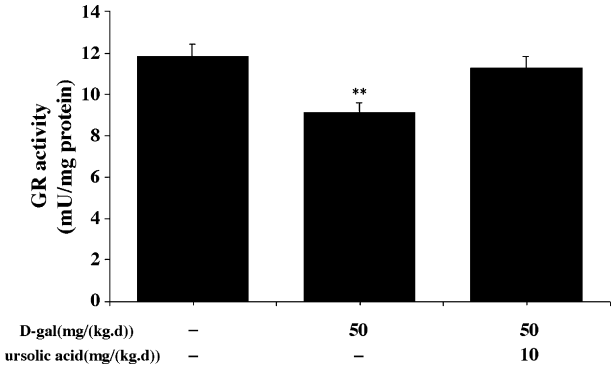

Fig. 6 – Effect of ursolic acid on the GR activity in the brain of D-gal-treated mice. Each value is the mean ± S.E.M. $^{**}P < 0.01$, as compared to the control group.

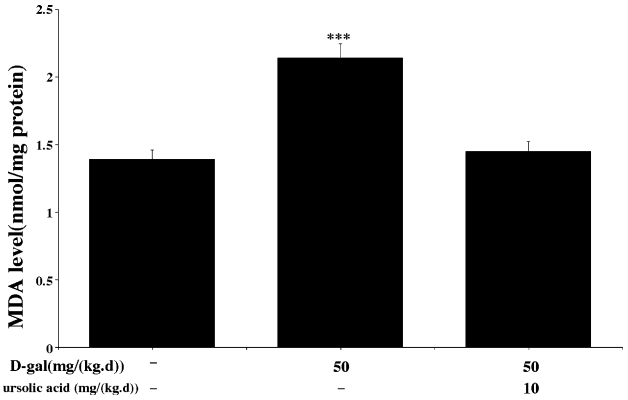

Fig. 7 – Effect of ursolic acid on the content of MDA in the brain of D-gal-treated mice. Each value is the mean ± S.E.M. $^{***}P < 0.001$, as compared to the control group.

2.7. *Western blot analysis*

Total protein extracts were prepared in 3 ml of ice cold RIPA lysis buffer [1 × TBS, 1% NP-40, 0.5% sodium deoxycholate, 0.1% SDS, 0.004% sodium azide] combining 30 μl of 10 mg/ml PMSF solution, 30 μl of Na_3VO_4 and 30 μl of protease inhibitors cocktail per gram of tissue. Lysates were centrifuged at 10,000 × *g* for 10 min at 4 °C, and then remove the supernatants and centrifuge again. The supernatants were collected. Protein levels in the supernatants were determined using the BCA assay kit (Pierce Biotechnology, Inc., Rockford, IL, USA). Samples (60 μg each) were separated by denaturing SDS-PAGE and transferred to a PVDF membrane (Roche Diagnostics Corporation) by electrophoretic transfer. The membrane was pre-blocked with 5% non-fat milk and 0.1% Tween-20 in Tris-buffered saline (TBS), incubated overnight

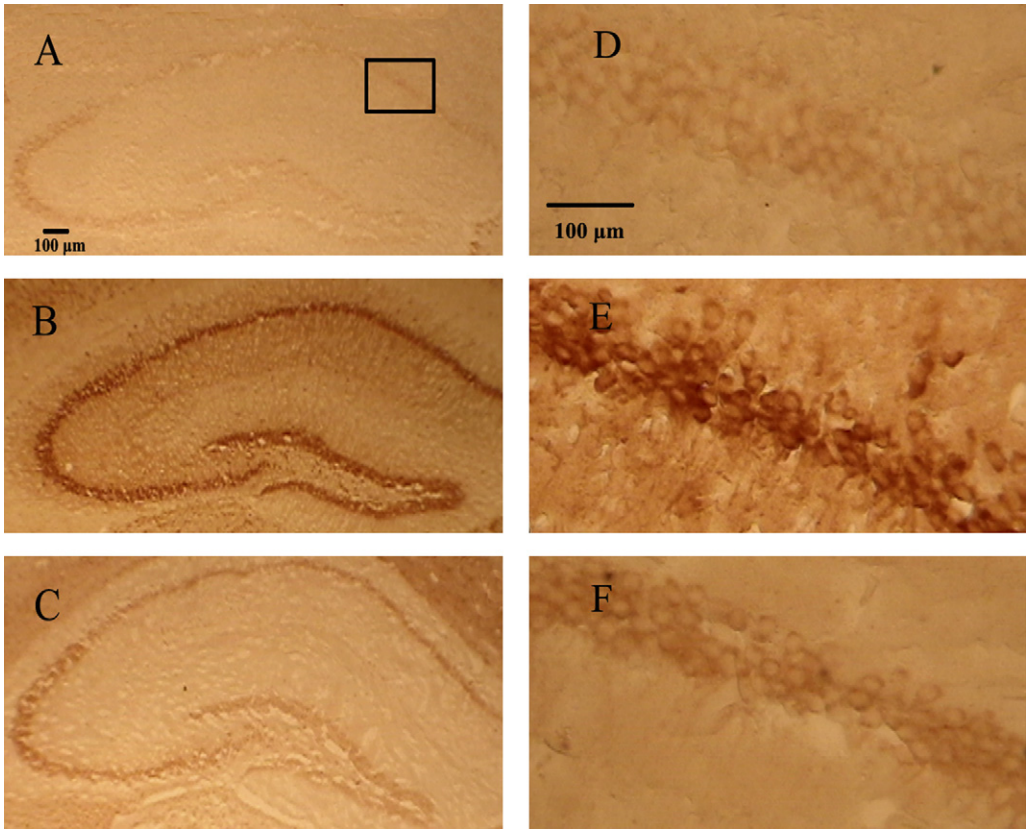

Fig. 8 – Immunohistochemistry analysis of cleaved caspase-3 in the hippocampus of mice. (A) The vehicle control mice; (B) D-gal-treated mice; (C) D-gal-treated mice fed with UA. The areas indicated within the boxes in panels A–C were enlarged in panels D–F for clearer visualization. Scale bars: 100 μm (A–F).

with either polyclonal rabbit anti-cleaved caspase-3 antibody (1:2000, Cell Signaling Technology, Inc., Beverly, MA, USA) or polyclonal rabbit anti-GAP43 antibody (1:1000, Chemicon International Inc., Temecula, CA). Quantitation of detected bands was performed with the Scion Image analysis software (Scion Corp., Frederick, MD, USA). Each density was normalized using each corresponding β-actin density as an internal control and we standardized the density of vehicle control for relative comparison as 1.0 to compare other groups.

2.8. *Statistic analysis*

All statistical analyses were performed using the SPSS software, version 11.5. Analysis of variance (ANOVA) was carried out with Newman–Keuls or Tukey's HSD post hoc test for multiple comparisons. Data were expressed as means ± S.E.M. Statistical significance was set at $P < 0.05$.

3. Results

3.1. *Effects of ursolic acid on the behaviour of D-gal-treated mice*

3.1.1. *Open field*

Based on spontaneous exploration of a novel environment, the open field is one of the most widely used behavioral tests. Fig. 1 shows that daily injection of D-gal produced behavioral effects in mice. These behavioral effects included decreased activity in the open-field, in terms of line crossing ($F(2, 27) = 5.198$,

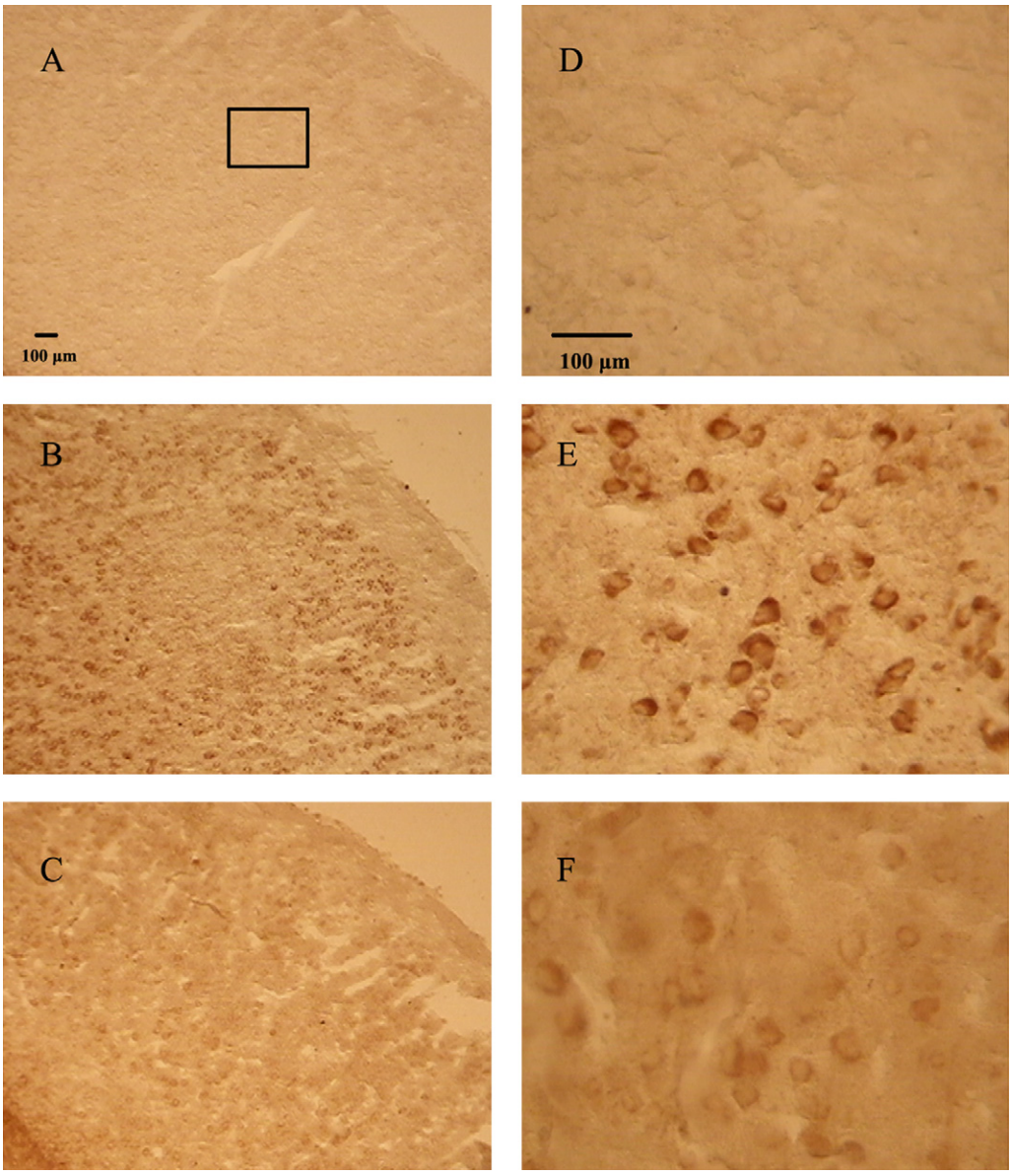

Fig. 9 – Immunohistochemistry analysis of activated caspase-3 in the cerebral cortex of mice. (A) The vehicle control mice; (B) D-gal-treated mice; (C) D-gal-treated mice fed with UA. The areas indicated within the boxes in panels A–C were enlarged in panels D–F for clearer visualization. Scale bars: 100 μm (A–F).

$P < 0.05$), rearing/leaning ($F(2, 27) = 16.598$, $P < 0.001$) and grooming ($F(2, 27) = 7.550$, $P < 0.01$). After 8 weeks of injection of D-gal, mice were fed with UA for another 2 weeks. No statistically significant difference was found between the vehicle and UA group.

3.1.2. *Morris water maze*

The Morris water maze is a sensitive method for revealing the impairment of spatial learning and memory. During the hidden sessions, all treated groups improved their performance with training. Compared to the vehicle, the D-gal group displayed increased latency to the platform (Fig. 2A). However, there was no significant difference in spatial learning ability between the vehicle controls and the UA-treated D-gal mice learned to find the hidden platform. In the probe trial following the last day of hidden platform training, D-gal-treated group made less platform crossings than the vehicle-treated group ($F(2, 27) = 4.559$, $P < 0.01$) and the UA treatment could increase the number of times of crossing over the platform site (Fig. 2B). Both vehicle-treated and UA-treated mice spent most of their time in the target quadrant where the platform had been located during the training (Fig. 2C). On the other hand, D-gal-treated group showed a decreased spatial preference for the target quadrant as compared with the vehicle.

3.2. *Effects of ursolic acid on antioxidative status of D-gal-treated mouse brain*

The concentration of ROS is determined by the balance between the rate of production and the rate of clearance by various antioxidant compounds and enzymes. Cu–Zn superoxide dismutase (Cu, Zn-SOD) is the first enzyme of the enzymatic antioxidative pathway to convert superoxide anions into peroxides, which are converted into water by catalase (CAT) and glutathione peroxidase (GPx). In the glutathione peroxide reaction, glutathione is oxidized into glutathione disulfide, which can be converted back to glutathione by glutathione reductase (GR) in an NADPH-consuming process [23,24]. To determine whether the increased oxidative damages in the brain of D-gal-treated mice is related to an altered antioxidant capacity, we measured the activities of major antioxidant enzymes in mouse brain. Figs. 3–6 present activities of antioxidant enzymes, including Cu, Zn-SOD, CAT, GPx, and GR, in the brain of mice. In D-gal-treated mice, Cu, Zn-SOD ($P < 0.001$), CAT ($P < 0.01$), GPx ($P < 0.01$) and GR ($P < 0.01$) activities decreased significantly as compared with those in the vehicle controls. In contrast, no significant decrease in activities of these antioxidant enzymes was observed in D-gal-treated mice fed with ursolic acid.

3.3. *Effects of ursolic acid on lipid peroxidation level in D-gal-treated mouse brain*

Our results in Fig. 7 demonstrated that the level of MDA in the brain of D-gal-treated mice was significantly higher than that in the vehicle control mice ($P < 0.001$). There was no significant difference with regard to the MDA content between ursolic acid-fed mice and the vehicle controls. The increase in lipid peroxidation indicates an elevated in vivo oxidative stress in the brain of D-gal-treated mice. Interestingly, ursolic acid could attenuate D-gal induced MDA increasing ($P < 0.001$).

3.4. *Effects of ursolic acid on the activation of caspase-3 in D-gal -treated mouse brain*

In our present study (Figs. 8 and 9) showed that D-gal treatment induced an increase in the activation of caspase-3 in both the hippocampus and cortex, which was reversed by ursolic acid. Western blot analysis also showed the activation of caspase-3 was induced by D-gal and was reversed by ursolic acid (Fig. 10).

3.5. *Effects of ursolic acid on the expression of the growth associated protein 43 mRNA in the D-gal-treated mouse brain*

Previous in situ analysis showed that the expression of the GAP43 gene was present in the hippocampus and the cortex of mice brain [25–27]. We examined the expression of GAP43 mRNA in these brain tissues by in situ hybridization (Figs. 11 and 12). For GAP43 mRNA, intense hybridization signals were detected only in the CA1, CA2, and CA3 regions of the hippocampus (Fig. 11). Fig. 11 shows that the expression of GAP43 mRNA was decreased in the hippocampus of D-gal-treated mice brain. However, as compared to the D-gal-treated mice, a significantly increase of GAP43 mRNA level was found in the CA1, CA2, and CA3 regions of hippocampus in the D-gal-treated mice fed with ursolic acid. Similarly, the ursolic acid treatment also significantly restored the GAP43 mRNA expression in the cerebral cortex that was significantly decreased in the D-gal-treated mice (Fig. 12). Western blot analysis was also used to investigate the effect of ursolic acid

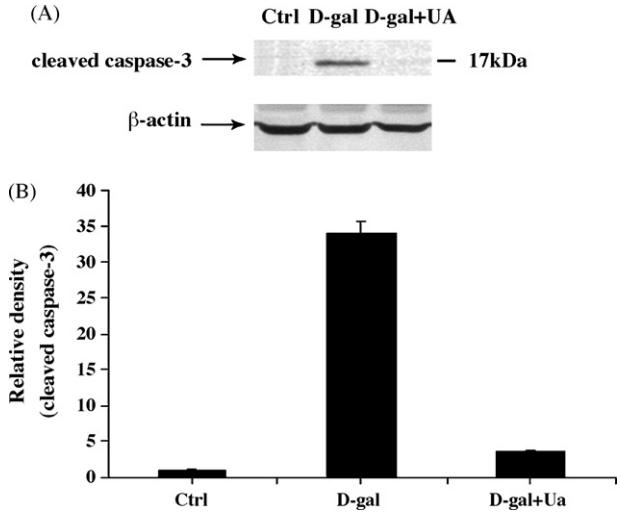

Fig. 10 – Western blot analysis of the activation of caspase-3 in the mouse brain. (A) A representative Western blot of the cleaved caspase-3 in vehicle control, D-gal-treated, and D-gal/UA-treated mice; (B) relative density analysis of the cleaved caspase-3 protein bands. β-Actin was probed as an internal control. The relative density is expressed as cleaved caspase-3/β-actin ratio and the vehicle control is set as 1.0. Values are averages from three independent experiments. Each value is the mean ± S.E.M.

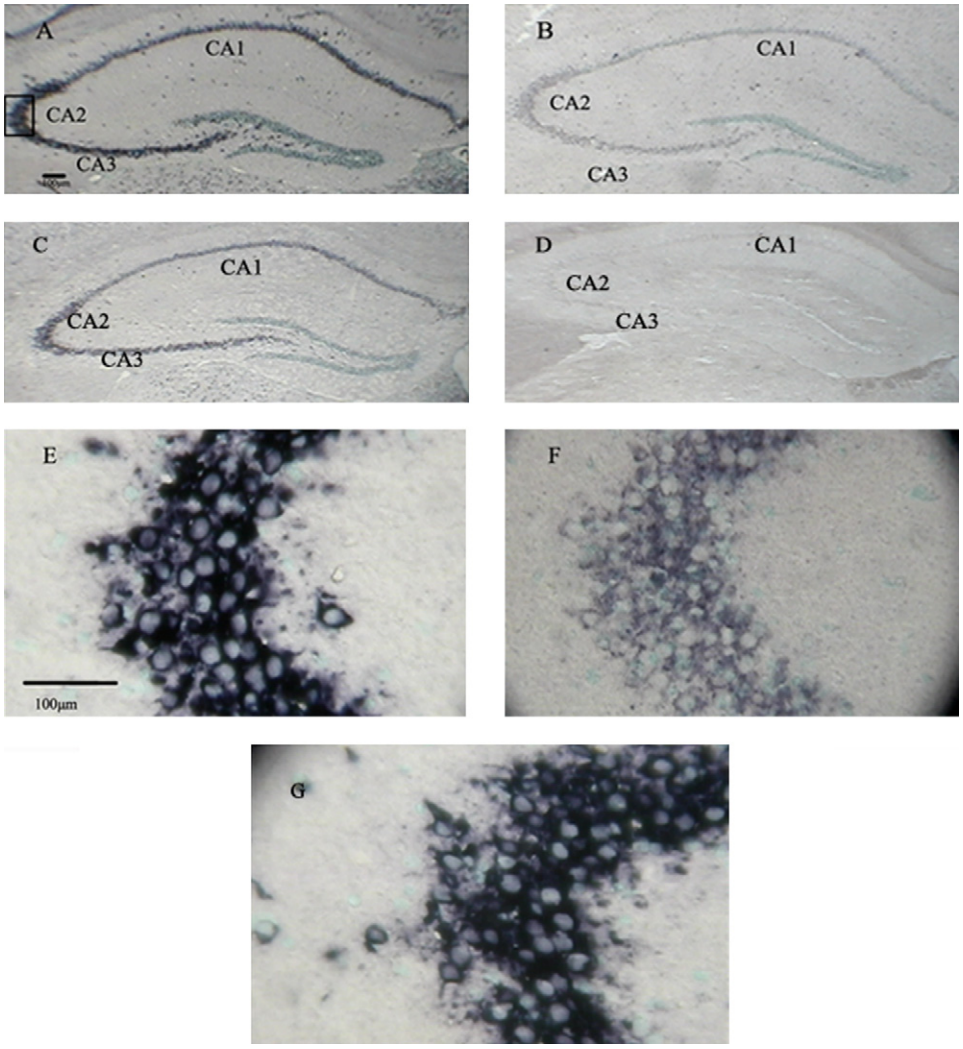

Fig. 11 – In situ hybridization analysis of the expression of GAP43 mRNA in the hippocampus of mice. Neuron-specific localization of GAP43 mRNA was detected with the antisense riboprobe (A–C, E–G), but no signal was detected with the sense riboprobe (D). (A) The vehicle control mice; (B) D-gal-treated mice; (C) D-gal-treated mice fed with UA. The areas indicated within the boxes in panels A–C were enlarged in panels E–G for clearer visualization. Sense RNA was used as a negative control (D). Scale bars: 100 μm (A–G).

on the expression of GAP43. Fig. 13 showed that D-gal significantly reduced the expression of GAP43 and ursolic acid induced it in the mouse brain.

4. Discussion

The increase in life expectancy in the 21st century has resulted in an increase in the prevalence of age-dependent diseases such as depression, Alzheimer's disease (AD) and other dementias. A number of studies have been carried out to seek new therapies, especially focusing on the aging process itself. It is important to identify the adverse effects of age-related changes and develop therapies that retard or reverse such changes. Because D-gal has a neurotoxic effect, different animal species injected with D-gal have been used as aging models for brain aging or anti-aging pharmacological studies [28,29]. In our study, we first investigated the effects of ursolic acid on the D-gal-induced neurotoxicity by behavioral tests. Significant differences between the vehicle and D-gal-treated mice were observed in the open field test, suggesting that the injection of D-gal causes motor abnormalities and impairments of novelty-induced exploratory behaviors (Fig. 1). The data also indicate that UA-feeding for 2 weeks is capable of reversing the D-gal induced behavioral impairment. The protective effect of UA on D-gal induced spatial learning and memory impairment was also demonstrated in water Maze test (Fig. 2).

On the other hand, D-gal causes age-related changes in different animal models. It has been reported that free radicals were increased in D-gal-treated animals and the free radical theory of aging indicates that these increased free radicals may account for the underlining mechanism responsible for age-related degenerative processes [28,30–33]. The cellular redox homeostasis could be maintained by the production of

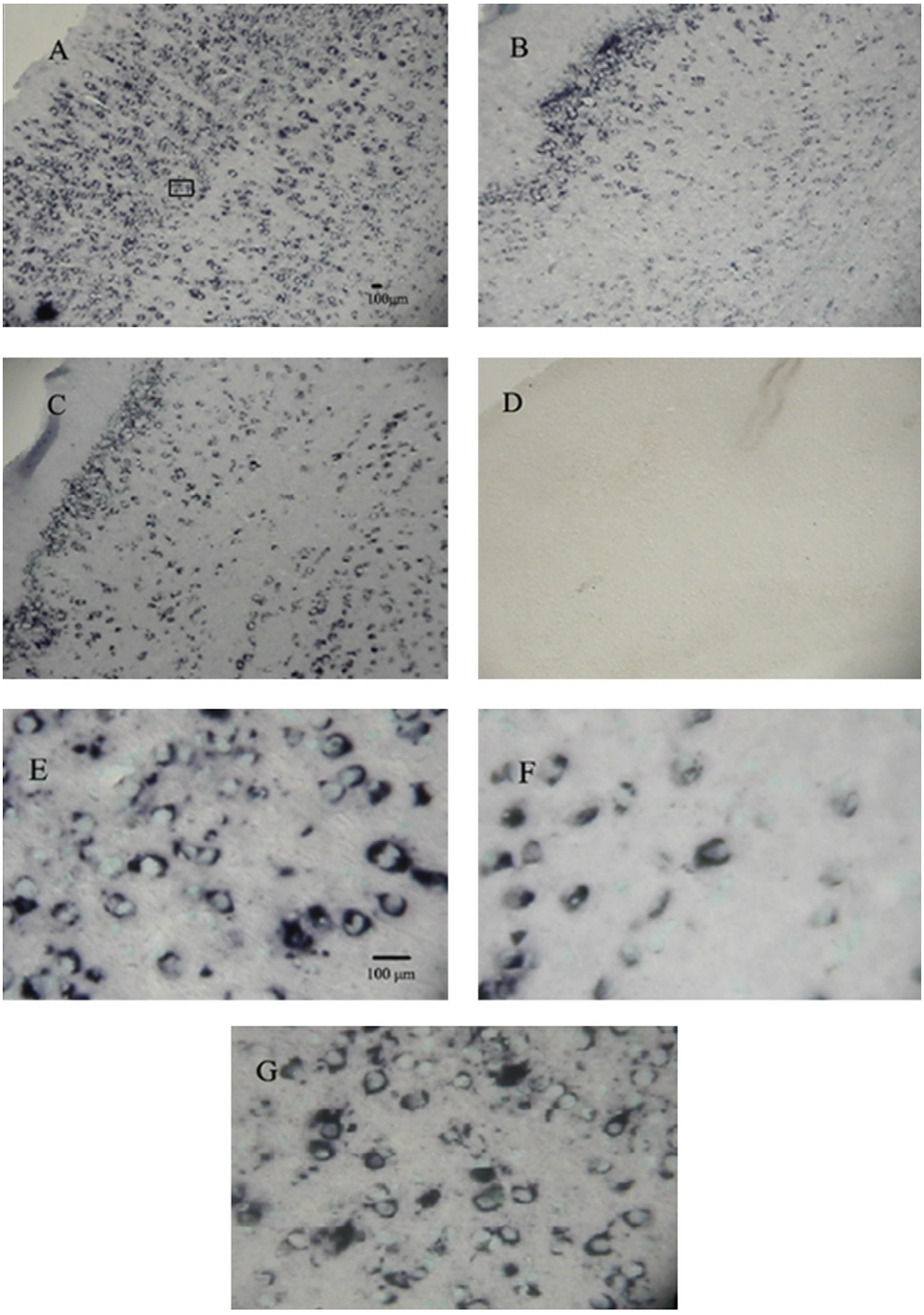

Fig. 12 – In situ hybridization analysis of the expression of GAP43 mRNA in the cerebral cortex of mice. Neuron-specific localization of GAP43 mRNA was detected with the antisense (A–C, E–G) riboprobe, but no signal was detected with the sense riboprobe (D). (A) The vehicle control mice; (B) D-gal-treated mice; (C) D-gal-treated mice fed with UA. The areas indicated within the boxes in panels A–C were enlarged in panels E–G for clearer visualization. Sense RNA was used as a negative control (D). Scale bars: 100 μm (A–G).

ROS and the activities of antioxidant enzymes. An extended life span was also observed in *Drosophila* strains with extra copies of genes encoding SOD and catalase [34,35]. In our study, the activities of antioxidative enzymes, including CAT, SOD, GPx, and GR were measured in mouse brain. As lipid peroxidation induced by ROS may also contribute to the neurotoxicity in mouse brain, the ROS production could be indirectly estimated by measuring MDA, a product of lipid

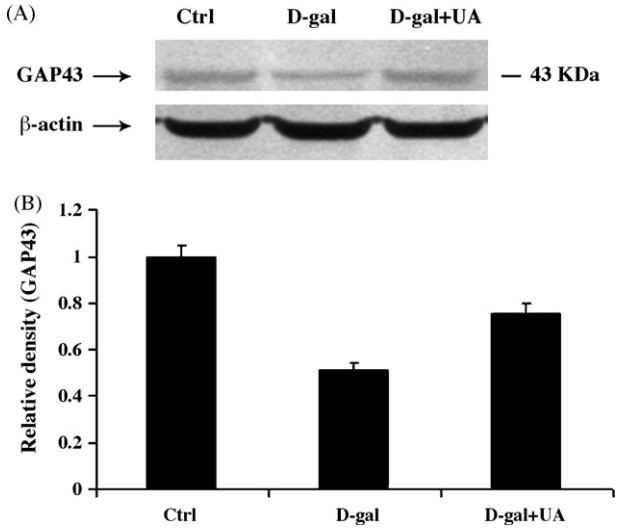

Fig. 13 – Western blot analysis of the expression of GAP43 in the mouse brain. (A) A representative Western blot of GAP43 in vehicle control, D-gal-treated, and D-gal/UA-treated mice; (B) relative density analysis of the cleaved GAP43 protein bands. β-Actin was probed as an internal control. The relative density is expressed as cleaved GAP43/β-actin ratio and the vehicle control is set as 1.0. Values are averages from three independent experiments. Each value is the mean ± S.E.M.

peroxidation. In the brain of D-gal-treated mice, lowered SOD, CAT, GPx, GR activities and elevated MDA content were observed as compared with the vehicle control mice, consistent with previous studies. Many studies indicated that UA has a potent antioxidant activity by scavenging free radicals [11]. The antioxidant activity of UA isolated from *Ocimum sanctum* against free radical induced damage was studied by Balanehru and Nagarajan [36]. UA was identified as inhibitor of O_2^- generation in xanthine (XA)-xanthine oxidase (XOD) assay system. It also showed marked inhibitory effects on the tumor promoter 12-O-tetradecanoylphorbol-13-acetate (TPA)-induced O_2^- generation in dimethylsulfoxide (DMSO)-differentiated HL-60 cells. Heo et al. [37] investigated the effect of UA from *Origanum majorana* L. on Abeta-induced neurotoxicity using PC12 cells. Pretreatment with isolated UA and Vitamin E prevented the PC12 cell from ROS toxicity, which is mediated by Aβ. This study suggested that UA might be an effective therapeutic agent in AD. Strikingly, UA significantly increased the activities of all these enzymes and decreased the level of MDA in the brain of D-gal-treated mice (Figs. 3–7). Our results strongly suggest that UA can strengthen antioxidative defence against free radicals induced by D-gal in vivo.

In addition, age-related changes in neuronal function, viability and ultimately cognition are attributable to the cell death resulted from oxidative damages [38,39]. Many evidences showed that ROS-mediated increase in the activation of caspase-3 could result in impaired neuronal function and, eventually, neurodegeneration [40,41]. Considering the roles of caspase-3, an effector caspase, in the process of cell death, we measured the cleaved caspase-3 in the brain of mice. Our results revealed that D-gal induced neurotoxic effects were associated with the activation of caspase-3. D-gal induced the activation of caspase-3 was reversed by treatment of UA in mouse brain (Figs. 8 and 9). Western blot analysis also showed ursolic acid could significantly reverse the activation of caspase-3 in the D-gal-treated mice.

The neural growth-associated protein GAP43 is thought to play a role in axonal elongation, synaptic plasticity, and nerve sprouting during development and in adult [42–46]. Although the precise role of this protein in the adult nerve system is not yet known, several lines of evidence relate the level of GAP43 mRNA to structural synaptic plasticity in the adult nervous system [47,48]. To this end we have used in situ hybridization techniques to study the distribution and the level of GAP43 mRNA in the hippocampus and the cerebral cortex of mice (Figs. 11 and 12). The expression of GAP43 mRNA was observed in the CA1, CA2, CA3 regions of hippocampus and the cerebral cortex. UA could restore the expression of GAP43 mRNA in the hippocampus and the cerebral cortex of mice treated with D-gal. In considering the level of GAP43 mRNA elevated by UA, it should be emphasized that it may be required in the structural synaptic reorganization of the injured neurons. This possibility is supported by the reversal effect of ursolic acid on D-gal induced learning and memory impairment (Fig. 13).

In conclusion, UA, a pentacyclic triterpene acid, has an effectively antioxidative activity. Our present study showed that ursolic acid could reverse the neurotoxic effect in mice brain induced by D-gal, through (1) elevating antioxidant enzymes activities and reducing MDA content, (2) reducing the activation of caspase-3, and (3) restoring GAP43 expression.

Acknowledgements

This work is supported by the Major Fundamental Research Program of Natural Science Foundation of he Jiangsu Higher Education Institutions of China (2007), Foundation for University Key Teacher by the Ministry of Education of PR China, Grants from Key Laboratory of Jiangsu Province, Grants from Natural Science Foundation by Xuzhou Normal University (05XLA14) and Grants from Qing Lan Project of Jiangsu Province, PR China.

REFERENCES

[1] Olanow CW. A radical hypothesis for neurodegeneration. Trends Neurosci 1993;16(11):439–44.
[2] Castegna A, Aksenov M, Aksenova M, Thongboonkerd V, Klein JB, Pierce WM, et al. Proteomic identification of oxidatively modified proteins in Alzheimer's disease brain. Part I: creatine kinase BB, glutamine synthase, and ubiquitin carboxy-terminal hydrolase L-1. Free Radic Biol Med 2002;33(4):562–71.
[3] De Iuliis A, Grigoletto J, Recchia A, Giusti P, Arslan P. A proteomic approach in the study of an animal model of Parkinson's disease. Clin Chim Acta 2005;357:202–9.
[4] Zhang Q, Li X, Cui X, Zuo P. D-Galactose injured neurogenesis in the hippocampus of adult mice. Neurol Res 2005;27(5):552–6.

[5] Wei HF, Li L, Song QJ, Ai HX, Chu J, Li W. Behavioural study of the d-galactose induced aging model in C57BL/6J mice. Behav Brain Res 2005;157:245–51.
[6] Cui X, Zuo P, Zhang Q, Li X, Hu Y, Long J, et al. Chronic systemic D-galactose exposure induces memory loss, neurodegeneration, and oxidative damage in mice: protective effects of R-alpha-lipoic acid. J Neurosci Res 2006;83(8):1584–90.
[7] Chen JH, Xia ZH, Tan RX. High-performance liquid chromatographic analysis of bioactive triterpenes in Perilla frutescens. J Pharm Biomed Anal 2003;32:1175–9.
[8] Tokuda H, Ohigashi H, Koshimizu K, Ito Y. Inhibitory effects of ursolic and oleanolic acid on skin tumor promotion by 12-O-tetradecanoylphorbol-13-acetate. Cancer Lett 1986;33:279–85.
[9] Liu J. Pharmacology of oleanolic acid and ursolic acid. J Ethnopharmacol 1995;49(2):57–68.
[10] Mahato SB, Sarkar SK, Poddar G. Triterpenoid saponins. Phytochemistry 1988;27:3037–67.
[11] Kim JS, Huh JI, Song SH, Shim KH, Back BS, Kim KW, et al. The antioxidative mechanism of ursolic acid. J Gastroenterol 1996;6:52–6.
[12] Shishodia S, Majumdar S, Banerjee S, Aggarwal BB. Ursolic acid inhibits nuclear factor-κB activation induced by carcinogenic agents through suppression of IκBα kinase and p65 phosphorylation: correlation with down-regulation of cyclooxygenase 2, matrix metalloproteinase 9, and cyclin D1. Cancer Res 2003;63:4375–83.
[13] Murakamia S, Takashimaa H, Sato-Watanabea M, Chonana S, Yamamotoa K, Saitoha M, et al. Ursolic acid, an antagonist for transforming growth factor (TGF)-beta1. FEBS Lett 2004;566:55–9.
[14] Shukla B, Visen PKS, Patnaik GK, Tripathi SC, Srimal RC, Dayal R, et al. Hepatoprotective activity in the rat of ursolic acid isolated from Eucalyptus hybrid. Phytother Res 1992;6(2):74–9.
[15] Saravanan R, Viswanathan P, Pugalendi KV. Protective effect of ursolic acid on ethanol-mediated experimental liver damage in rats. Life Sci 2006;78:713–8.
[16] Shih YH, Chein YC, Wang JY, Fu YS. Ursolic acid protects hippocampal neurons against kainate-induced excitotoxicity in rats. Neurosci Lett 2004;362:136–40.
[17] Wang R, Zhang HY, Tang XC, Huperzine. A attenuates cognitive dysfunction and neuronal degeneration caused by beta amyloid protein-(1–40) in rat. Eur J Pharmacol 2001;421:149–56.
[18] McCord JM, Fridowich I. An enzymic function for erythrocuprein. J Biol Chem 1969;244:6049–55.
[19] Aebi H. Catalase in vitro. Methods Enzymol 1984;105: 121–7.
[20] Paglia DE, Valentine WN. Studies on the quantitative and qualitative characterization of erythrocyte glutathione peroxidase. J Lab Clin Med 1967;70:158–69.
[21] Mizumo Y, Ohta K. Regional distributions of thiobarbituric acid reactive products, activities of enzymes regulating the metabolism of oxygen free radicals, and some of the related enzymes in adult and aged rat brain. J Neurochem 1986;46:1344–52.
[22] Uchiyama M, Mihara M. Determination of Malondialdehyde precursor in tissues by thiobarbituric acid test. Anal Biochem 1978;86:271–8.
[23] Deby C, Goutier R. New perspectives on the biochemistry of superoxide anion and the efficiency of superoxide dismutases. Biochem Pharmacol 1990;39:399–405.
[24] Halliwell B, Gutteridge JMC, editors. Free radicals in biology and medicine. second ed., Oxford, UK: Clarendon; 1989.
[25] Higo N, Oishi T, Yamashita A, Matsuda K, Hayashi M. Gene expression of growth-associated proteins, GAP-43 and SCG10, in the hippocampus formation of the macaque monkey: nonradioactive in situ hybridization study. Hippocampus 1998;8:533–47.
[26] Jacobs KM, Neve RL, Donoghue JP. Neocortex and hippocampus contain distinct distributions of calcium-calmodulin protein kinase II and GAP43 mRNA. J Comp Neurol 1993;336(1):151–60.
[27] Higo N, Oishi T, Yamashita A, Matsuda K, Hayashi M. Quantitative non-radioactive in situ hybridization study of GAP-43 and SCG10 mRNAs in the cerebral cortex of adult and infant macaque monkeys. Cereb Cortex 1999;9(4): 317–31.
[28] Ho SC, Liu JH, Wu RY. Establishment of the mimetic aging effect in mice caused by D-galactose. Biogerontology 2003;4:15–8.
[29] Zhang C, Wang SZ, Zuo PP, Cui X, Cai J. Protective effect of tetramethylpyrazine on learing and memory function in D-galactose-lesioned mice. Chin Med Sci J 2004;19(3):180–4.
[30] Shen YX, Xu SY, Wei W, Sun XX, Yang J, Liu LH, et al. Melatonin reduces memory changes and neural oxidative damage in mice treated with D-galactose. J Pineal Res 2002;32(3):173–8.
[31] Zhang X, Zhang BZ, Yang XL, Zhang WW, Li L. Behavior and memory changes in D-galactose-induced aging rat model. Chin J Gerontol 1996;16:230–2.
[32] Multhaup G, Ruppert T, Schlicksupp A, Hesse L, Beher D, Masters CL, et al. Reactive oxygen species and Alzheimer's disease. Biochem Pharmacol 1997;54:533–9.
[33] Harman D. Aging: a theory based on free radical and radiation chemistry. J Gerontol 1956;11:298–300.
[34] Orr WC, Sohal RS. Extension of lifespan by overexpression of superoxide dismutase and catalase in *Drosophis melanogaster*. Science 1994;263:1128–30.
[35] Parkes TL, Elia AJ, Dickinson D, Hilliker AJ, Boulianne GL, John P. Extension of *Drosophila* lifespan by overexpression of human SOD1 in motorneurons. Nat Genet 1998;19: 171–4.
[36] Balanehru S, Nagarajan B. Protective effect of oleanolic acid and ursolic acid against lipid peroxidation. Biochem Int 1991;24:981–90.
[37] Jiwajinda S, Santisopasri V, Murakami A, Kim OK, Kim HW, Ohigashi H. Suppressive effects of edible Thai plants on superoxide and nitric oxide generation. Asian Pac J Cancer Prev 2002;3:215–23.
[38] Mattson MP. Pathways towards and away from Alzheimer's disease. Nature 2004;430(7000):631–9.
[39] Retter RJ, Tan DX, Pappolla MA. Melatonin relieves the neural oxidative burden that contributes to dementias. Ann N Y Acad Sci 2004;1035:179–96.
[40] Ozdener H. Molecular mechanisms of HIV-1 associated neurodegeneration. J Biosci 2005;30(3):391–405.
[41] Schon EA, Manfredi G. Neuronal degeneration and mitochondrial dysfunction. J Clin Invest 2003;111(3): 303–12.
[42] Bisby MA, Tetzlaff W. Changes in cytoskeletal protein synthesis following axon injury and during axon regeneration. Mol Neurobiol 1992;6(2–3):107–23.
[43] Verhaagen J, Oestreicher AB, Gispen WH, Margolis FL. The expression of the growth associated protein B50/GAP43 in the olfactory system of neonatal and adult rats. J Neurosci 1989;9:683–91.
[44] Frey D, Laus T, Xu L, Schneider C, Caroni P. Shared and unique roles of GAP23 and GAP43 in actin regulation, neurite outgrowth, and anatomical plasticity. J Cell Biol 2000;149(7):1443–53.
[45] Rosenbrock H, Koros E, Bloching A, Podhorna J, Borsini F. Effect of chronic intermittent restraint stress on hippocampal expression of marker proteins for synaptic plasticity and progenitor cell proliferation in rats. Brain Res 2005;1040:55–63.

[46] Aigner L, Arber S, Kapfhammer JP, Laux T, Schneider C, Botteri F, et al. Overexpression of the neural growth-associated protein GAP-43 induces nerve sprouting in the adult nervous system of transgenic mice. Cell 1995;83:269–78.
[47] Capone GT, Bendotti C, Oster-Granite ML, Coyle JT. Developmental expression of the gene encoding growth-associated protein 43 (Gap43) in the brains of normal and aneuploid mice. J Neurosci Res 1991;29(4): 449–60.
[48] Kwon BK, Liu J, Oschipok L, Teh J, Liu ZW, Tetzlaff W. Rubrospinal neurons fail to respond to brain-derived neurotrophic factor applied to the spinal cord injury site 2 months after cervical axotomy. Exp Neurol 2004;189:45–57.